An Erbium Fiber Laser With Single-Frequency Oscillation and Wavelength-Upconverted Output
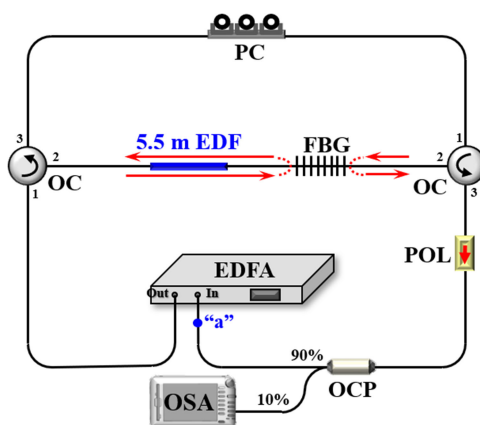
Chien-Hung Yeh
Wei-Yao You
Jhao-Ren Chen
Chi-Wai Chow
Wen-Piao Lin

An Erbium Fiber Laser With Single-Frequency Oscillation and Wavelength-Upconverted Output

Chien-Hung Yeh [ID],[1] **Wei-Yao You** [ID],[1] **Jhao-Ren Chen** [ID],[1]
Chi-Wai Chow [ID],[2] **and Wen-Piao Lin** [ID][3,4]

[1]Department of Photonics, Feng Chia University, Taichung 40724, Taiwan
[2]Department of Photonics and Institute of Electro-Optical Engineering, National Chiao Tung University, Hsinchu 30010, Taiwan
[3]Department of Electrical Engineering, Chang Gung University, Taoyuan 33302, Taiwan
[4]Department of Holistic Medicine, Linkou Chang Gung Memorial Hospital, Taoyuan 33302, Taiwan

Abstract: In this paper, we present experimentally an erbium-doped fiber (EDF) laser system to accomplish the single-longitudinal-mode (SLM) and wavelength-upconverted output by using nonlinear effect. To accomplish the SLM output, a short length of unpumped EDF saturable absorber (SA) is applied inside the EDF laser cavity for filtering densely multi-mode noise. In accordance with the designed EDF laser system, the lasing wavelength can be upconverted to a longer wavelength position. In addition, the output characteristics of output power, optical signal to noise ratio (OSNR), tunability, stability and linewidth in the EDF laser are also discussed.

Index Terms: Fiber laser, erbium-doped fiber (EDF), wavelength-upconverted, single-longitudinal-mode (SLM).

1. Introduction

In recent times, erbium-doped finer (EDF) based gain medium in the fiber laser systems have attracted more interests due to their valuable applications in the optical communication, wavelength-division-multiplexing (WDM) traffic, micro-wave photonic, fiber sensing, high resolution spectroscopy and instrument testing [1]–[5]. Furthermore, the homogeneous broadening gain medium of EDF and longer fiber loop in the fiber laser would bring the unstable multi-longitudinal-mode (MLM) and mode-hopping output [6], [7]. Hence, in order to attain the single-longitudinal-mode (SLM) oscillation in the EDF based lasers, a number of techniques have been proposed and demonstrated, such as exploiting a unpumped EDF or graphene based saturable absorbers (SAs) [8], [9], using the multiple-ring architectures [10], [11], employing optical-injection loop design [12], [13], applying Mach-Zehnder interferometer (MZI) structure [14], [15], and utilizing the Rayleigh backscattering (RB) method [16], [17]. To accomplish the wavelength tunability in EDF lasers, different optical filters have been utilized inside the fiber cavity for selecting, such as the optical tunable
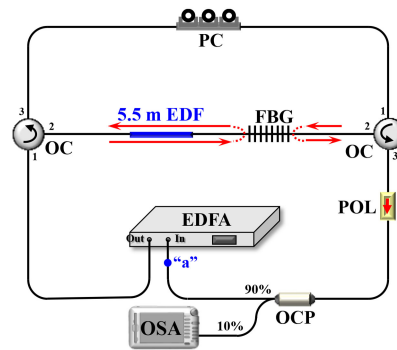
Fig. 1. Proposed wavelength-upconverted EDF ring laser configuration.

bandpass filter (OTBPF), ultra-narrow filter, Fabry-Perot tunable filter (FP-TF), Silicon-micro-ring resonator (SMRR) and fiber Bragg grating (FBG) [18]–[20]. Hence, the passband of each optical filter only could allow its corresponding wavelength output in the EDF laser for lasing.

In this work, we first demonstrate and execute an EDF ring laser diagram with a short length of EDF SA to reach SLM oscillation. Generally, we can apply the FBG inside the laser cavity to generate the corresponding wavelength based on its Bragg wavelength. However, based on the designed EDF laser scheme, the lasing wavelength can be upconverted to 1554.30, 1558.37 and 1562.83 nm owing to the nonlinear effect, while the original Bragg wavelength of FBG is selected at 1544.04, 1535.98 and 1531.79 nm, respectively. As the Bragg wavelength of FBG is at the shorter wavelength, the output wavelength can be upconverted to the longer wavelength. The output powers, optical signal to noise ratios (OSNRs) and laser linewidths of the proposed wavelength-upconverted EDF laser are −11.7, −4.8 and −3.5 dBm, 32.4, 33.5 and 32.8 dB, and 22, 23 and 28 kHz, respectively, at the three output wavelengths. Moreover, the output stabilities of power and wavelength are less than 0.4 dB and 0.3 nm during one-hour observation. In the experiment, we can also obtain the downconverted wavelength output depending on the smaller injected power for observation.

2. Experiment and Results

Fig. 1 schemes the proposed EDF laser architecture for upconverting output wavelength by nonlinear effect. The demonstrated EDF ring laser is constructed by a fiber Bragg grating (FBG), two optical circulators (OCs), a polarization controller (PC), a fiber-type polarizer (POL), an erbium-doped fiber amplifier (EDFA), a length of 5.5 m unpumped EDF and a 1×2 and 10:90 optical coupler (OCP). In the experiment, the commercial C-band EDFA, having the saturation power of 13 dBm, can be used to regard as the gain medium and also cause the nonlinear effect for generating the upconverted wavelength output. The obtainable gain bandwidth of EDFA is between 1528.0 and 1564.0 nm for utilization. The PC and POL are employed inside the fiber cavity to control the birefringence for maintaining the polarization direction and accomplishing the optimal output power. A length of 5.5 m unpumped EDF is exploited to act as saturable absorber (SA) for filtering the MLM oscillation [9]. Thus, the lasing wavelength of the EDF laser could reach the SLM performance. In addition, two OCs can cause the dual fiber ring cavity architecture, as shown in Fig. 1.

To understand the wavelength-upconverted output of proposed EDF laser configuration, we select three FBGs with various Bragg wavelength to produce different outputs. Here, the reflected wavelength of three FBGs are 1544.04 (FBG_1), 1535.89 (FBG_2) and 1531.79 nm (FBG_3), respectively, as illustrated in Fig. 2(a) to Fig. 2(c). The observed reflectivity of three FBGs are larger than 94%. Moreover, the 3 dB bandwidth of each FBG is measured at 0.19, 0.16 and 0.22 nm, as shown in Fig. 2(a) to Fig. 2(c). In the experiment, the FBG is used individually in the presented EDF laser configuration.
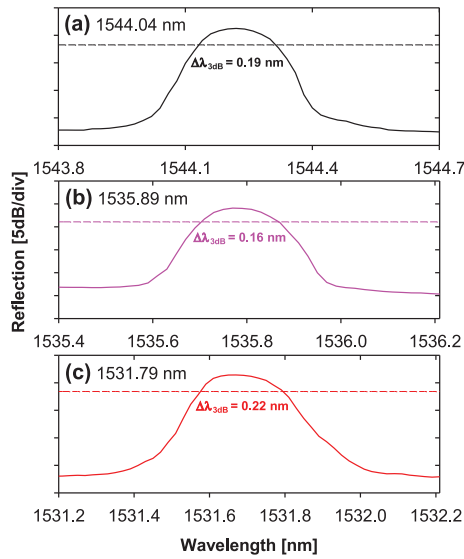
Fig. 2. Measured reflection spectra of FBG under the Bragg wavelength of (a) 1544.04, 1535.89, and 1531.79 nm, respectively.
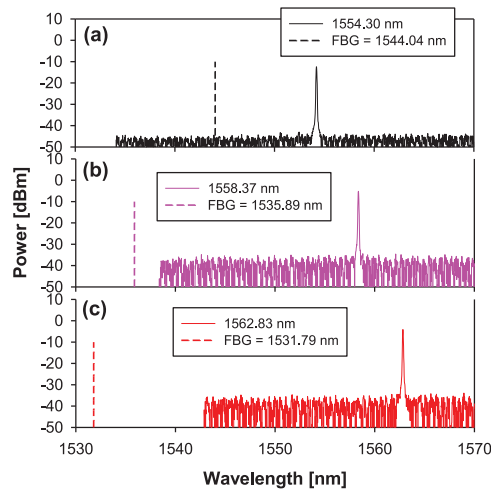

Fig. 3. Measured upconverted wavelengths of (a) 1554.30, (b) 1558.37, and (c) 1562.83 nm in the presented EDF laser, respectively.

Commonly, an FBG could be applied inside the EDF cavity to produce corresponding output wavelength based on its reflected Bragg wavelength in the previous studies [19], [21]. When we place the three FBGs with different Bragg wavelength inside the ring cavity individually, the output wavelength is measured as exhibited in Fig. 3(a) to Fig. 3(c), owing to the nonlinear effect in the presented EDF laser. The output wavelength can be upconverted to 1554.30, 1558.37 and 1562.83 nm, while the original Bragg wavelength of FBG is 1544.04, 1535.98 and 1531.79 nm, respectively. If the Bragg wavelength of FBG is at the shorter wavelength position, the lasing wavelength can be upconverted to the longer wavelength, as seen in Fig. 3. Moreover, the obtained optical signal to noise ratios (OSNRs) and output powers of three lasing wavelengths in the designed EDF laser are 32.4, 33.5 and 32.8 dB, and -11.7, -4.8 and -3.5 dBm, respectively. In the experiment, the resolution bandwidth (RBW) of OSA is set at 1 nm for OSNR measurement. As a result, we
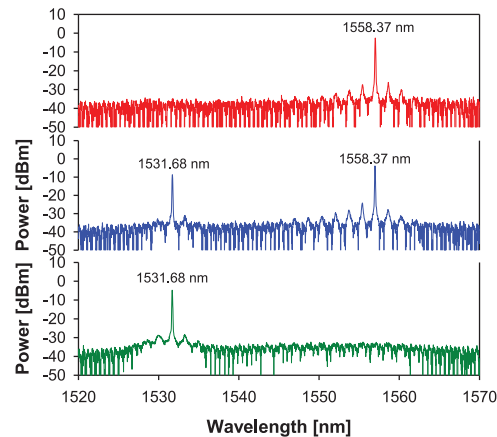
Fig. 4. Measured lasing wavelengths when the input power is (a) −12.3, (b) −14.4, and (c) −21.9 dBm at the "a" point, respectively.

can apply the presented EDF laser scheme for wavelength-upconverted operation by utilizing the different Bragg wavelength of FBGs inside the ring cavity.

To realize the operation mechanism of proposed EDF laser, using different injected power of lasing lightwave is also performed. Here, we cannot change the 980 nm pump power of commercial EDFA for gain control. Hence, the variable optical attenuator (VOA) and power meter (PM) are placed at the "a" point of Fig. 1 to control and observe the injected power of lasing wavelength. First, we utilize the FBG_2 (1535.89 nm) inside the ring loop of EDF laser for output measurement. The measured output wavelength can be upconverted to 1558.37 nm, when the injected power at "a" point is −12.3 dBm under original state, as shown in Fig. 4(a). Here, the up-converted wavelength will pass through the FBG_2 and not be reflected. Then, while we use the VOA to decrease the injected power to −14.4 dBm gradually, the observed optical spectrum will result in the dual-wavelength oscillation at 1531.68 and 1558.37 nm, as seen in Fig. 4(b). Next, we reduce the injected power to −21.9 dBm, the output spectrum is generated at the wavelength of 1531.72 nm, as displayed in Fig. 4(c). When we continue to reduce detected power at the "a" point, no lasing wavelength can be observed. In the demonstration, we cannot measure the output wavelength of around 1535.89 nm when the FBG_2 is applied in our proposed EDF laser system. Moreover, a smaller injected power would also cause the down-converted wavelength oscillation, as plotted in Fig. 4(b). As a result, while the injected power is −21.9 and −12.3 dBm at the "a" point of Fig. 1, respectively, the lasing wavelength could be observed at 1531.68 and 1558.37 nm. In the experiment, when we keep the EDF-SA and remove the FBG in the fiber laser configuration, the arbitrary and unstable wavelength output will be observed. Moreover, the observed physical behavior may be the nonlinear effect for up-converted oscillation based on the proposed EDF laser architecture.

In general, the output stability of EDF based laser is also important concern. Then, we will execute the output power variation of each lasing wavelength for the stability measurement. Fig. 5(a) presents the measured output power change of 1554.30, 1558.37 and 1562.83 nm under an observation time of 50 minutes, respectively. The largest output power variations of the proposed EDF laser are 0.2, 0.4 and 0.2 dB during a period of observation, respectively, as seen in Fig. 5(a). In addition, over one-hour detection, the power stabilities of three lasing wavelengths are kept within the same power variations.

Next, we also measure the wavelength fluctuation of the selected wavelength in the presented wavelength-upconverted EDF laser system. Fig. 5(b) illustrate the measured wavelength oscillations for 50 minutes observation, while the upconverted wavelengths are 1554.30, 1558.37 and 1562.83 nm, respectively. In the demonstration, the maximum wavelength oscillations of 0, 0 and
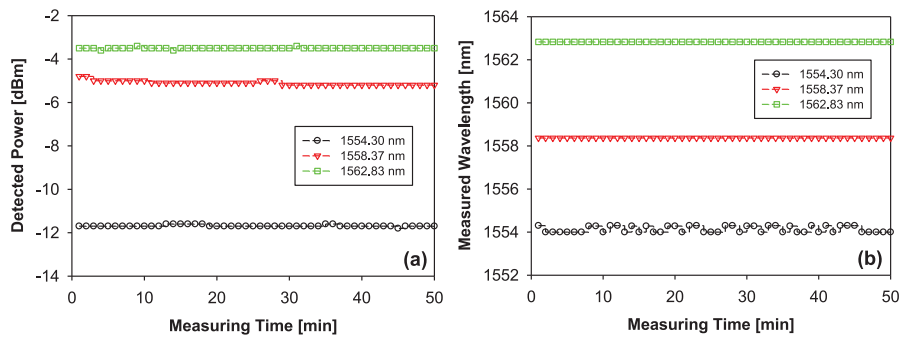
Fig. 5. (a) Observed output power change and (b) wavelength oscillations of 1554.30, 1558.37, and 1562.83 nm under an observation time of 50 minutes, respectively.
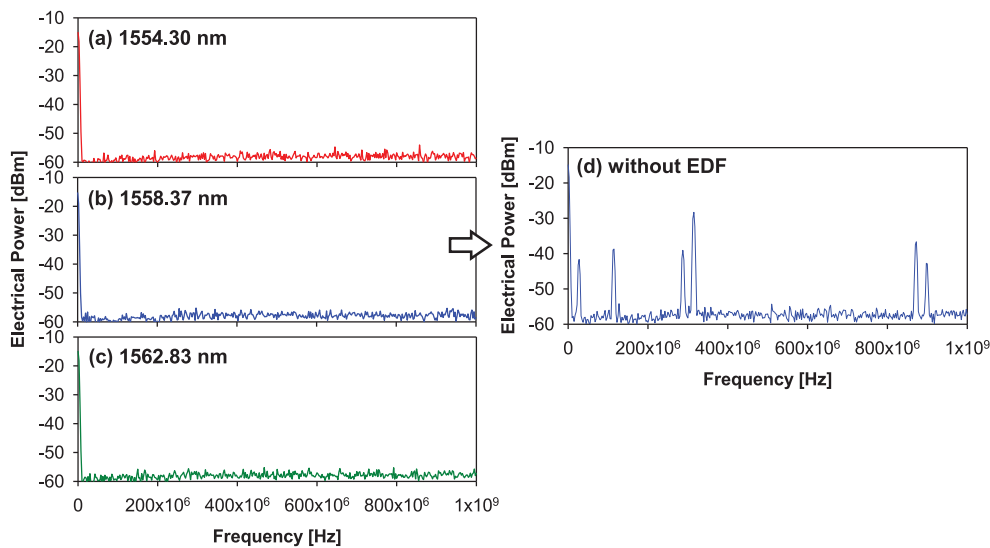

Fig. 6. Observed electrical spectra over the bandwidth of 1 GHz, while the lasing wavelengths of the EDF laser are (a) 1554.30, (b) 1558.37, and (c) 1562.83 nm, respectively. (d) The measured electrical spectrum at the wavelength of 1558.37 nm, when the 5.5 EDF is removed.

0.3 nm are observed in the same observing time, respectively. Through one hour observation, the maximum fluctuations of the three output wavelengths are also less than 0.3 nm. Therefore, the reached output stabilities of power and wavelength have the better performance in the proposed wavelength-upconverted EDF laser.

In accordance with the proposed EDF laser architecture, the lasing wavelength would pass through the 5.5 m EDF-SA twice, as seen in Fig. 1. To achieve the stable SLM operation, the EDF-SA can be applied to filter the dense MLM oscillation. Hence, we can exploit the delayed self-homodyne configuration for SLM demonstration. In the setup, two 1×2 and 50:50 OCPs, a PC and a length of 25 km fiber are used to construct the Mach-Zehnder interferometer (MZI) structure. Here, 25 km fiber is applied to act as the delay line for signal beating. Then, the beating wavelength is detected by a PIN receiver (Rx) to convert to electrical signal and observed by 3 GHz electrical spectrum analyzer (ESA). Fig. 6(a) to Fig. 6(c) present the observed electrical spectra over the bandwidth of 1 GHz, while the upconverted output wavelengths are 1554.30, 1558.37 and 1562.83 nm, respectively. We obtain that all the attained electrical spectra have no spike noises in the measured range of 1 GHz in the measurement, as seen in Fig. 6(a) to Fig. 6(c). Moreover,
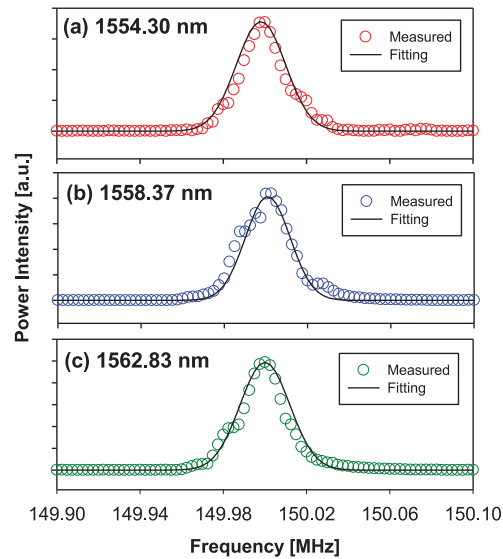
Fig. 7. Measured and fitted laser linewidth of proposed EDF laser, while the output wavelengths are (a) 1554.30, (b) 1558.37, and (c) 1562.83 nm, respectively.

the observed performance of SLM oscillation is also maintained over 50 minutes observing time. Therefore, we prove that the presented EDF laser has stable SLM output. The SLM operation of the proposed EDF laser is produced by applying the 5.5 m unpumped EDF based SA. The EDF SA would create standing wave effect to suppress the dense MLM [8]. When we use the FBG$_2$ and remove the EDF SA in the proposed fiber laser scheme, the observed side-mode could not be suppressed over the bandwidth of 0 to 1 GHz, as illustrated in Fig. 6(d). However, the measured output power and OSNR of lasing light are slightly larger than that of using EDF SA. Therefore, the EDF SA should be a key device for SLM operation. And the 5.5 m EDF based SA is the optimal length to reach the SLM output.

Subsequently, we also measure the laser linewidth of the three wavelengths. The delayed self-heterodyne linewidth measurement is also utilized. Here, we utilize the phase modulator (PM) in the other arm to generate the RF beating frequency of 150 MHz for signal detection. Thus, the corresponding linewidth of lasing wavelength is measured in the circle of Fig. 7(a) to Fig. 7(c), respectively. Then, we can apply the Lorentzian fitting curve to find the actual linewidth theoretically for the three measured wavelengths of 1554.30, 1558.37 and 1562.83 nm. Thus, the fitted line of 3 dB Lorentzian linewidth is 22, 23 and 28 kHz, respectively, as illustrated in Fig. 7(a) to Fig. 7(c).

3. Conclusion

We first designed and demonstrated an EDF ring laser scheme with a short length of EDF based SA to reach SLM operation. Commonly, the FBG was applied inside the laser cavity to generate the corresponding wavelength based on its Bragg wavelength. However, using the designed EDF ring laser configuration, the lasing wavelength could be upconverted to 1554.30, 1558.37 and 1562.83 nm owing to the nonlinear effect, while the original Bragg wavelength of FBG was nominated at 1544.04, 1535.98 and 1531.79 nm, respectively. As the Bragg wavelength of FBG was at the shorter wavelength, the output wavelength could be upconverted to the longer wavelength. The output powers, OSNRs and wavelength linewidths of the proposed wavelength-upconverted EDF laser were −11.7, −4.8 and −3.5 dBm, 32.4, 33.5 and 32.8 dB, and 22, 23 and 28 kHz, respectively, at the three output wavelengths. Additionally, the output stabilities of power and wavelength were fewer than 0.4 dB and 0.3 nm during one-hour observation. As the injected power of the lasing light gradually decreases, dual wavelength could be also achieved according to the designed EDF laser

configuration. When the injected power is below a certain level, the output wavelength would even be downconverted based on the experimental results. As a result, the demonstrated EDF laser scheme not only could reach upconverted and downconverted wavelength output, but also could accomplish SLM oscillation.

References

[1] H.-C. Lee, Y.-W. Lee, J.-S. Chang, and S.-K. Liaw, "Single-longitude-mode fiber laser implementation by using only two subring cavities in serial/parallel connection," *Fiber Integr. Opt.*, vol. 38, no. 4, pp. 236–246, 2019.

[2] H.-C. Chien, C.-H. Yeh, C.-C. Lee, and S. Chi, "A tunable and single-frequency S-band erbium fiber laser with saturable-absorber-based autotracking filter," *Opt. Commun.*, vol. 249, no. 1-3, pp. 261–264, 2005.

[3] S.-K. Liaw, Y.-W. Lee, H.-W. Huang, and W.-F. Wu, "Multi-wavelength linear-cavity SOA-based laser array for long-haul sensing," *IEEE Sens. J.*, vol. 15, no. 6, pp. 3353–3358, Jun. 2015.

[4] C.-H. Yeh and C.-W. Chow, "Broadband wavelength-tunable single-longitudinal-mode erbium-doped fiber ring laser using saturable-absorber filter," *Laser Phys. Lett.*, vol. 7, no. 2, pp. 158–163, 2010.

[5] Y.-H. Lin, C.-Y. Yang, J.-H. Liou, C.-P. Yu, and G.-R. Lin, "Using graphene nano-particle embedded in photonic crystal fiber for evanescent wave mode-locking of fiber laser," *Opt. Express*, vol. 21, no. 14, pp. 16763–16776, 2013.

[6] Y. Yao, X. Chen, Y. Dai, and S. Xie, "Dual-wavelength erbium-doped fiber laser with a simple linear cavity and its application in microwave generation," *IEEE Photon. Technol. Lett.*, vol. 18, no. 1, pp. 187–189, Jan. 2006.

[7] C.-H. Yeh, Y.-H. Zhuang, N. Tsai, C.-W. Chow, and J.-H. Chen, "Use of proper cavity loss for stable single-longitudinal-mode erbium fiber laser," *Laser Phys.*, vol. 27, no. 6, 2017, Art. no. 065109.

[8] S. H. Lee, H. G. Yun, M. H. Lee, S. H. Choi, and K. H. Kim, "Single-longitudinal-mode fiber ring lasers with a saturation-level-controlled saturable absorber," *Opt. Commun.*, vol. 308, pp. 15–19, 2013.

[9] F. D. Muhammad, M. Z. Zulkifli, A. A. Latif, S. W. Harun, and H. Ahmad, "Graphene-based saturable absorber for single-longitudinal-mode operation of highly doped erbium-doped fiber laser," *IEEE Photon. J.*, vol. 4, no. 2, Apr. 2012.

[10] C.-H. Yeh, Y.-R. Xie, C.-M. Luo, and Y. J.-Chang, "Widely 70-nm wavelength tunability single-frequency erbium laser utilizing multiple-ring architecture," *Opt. Laser Technol.*, vol. 120, 2019, Art. no. 105706.

[11] J. Zhang and J. W. Y. Lit, "Erbium doped fiber compound-ring laser with a ring filter," *IEEE Photon. Technol. Lett.*, vol. 6, no. 5, pp. 588–590, May 1994.

[12] C.-H. Yeh, T.-J. Huang, Z.-Q. Yang, C.-W. Chow, and J.-H. Chen, "Stable single-longitudinal-mode erbium fiber ring laser utilizing self-injection and saturable absorber," *IEEE Photon. J.*, vol. 9, no. 6, Dec. 2017, Art. no. 7106206.

[13] G.-R. Lin and J.-R. Wu, "The frequency dependent mode-locking behavior of an optical-injection-locked erbium-doped fiber laser," in *Proc. CLEO-PR*, 2003, pp. 1–2.

[14] M. I. Md Ali *et al.*, "Tapered-EDF-based Mach-Zehnder interferometer for dual-wavelength fiber laser," *IEEE Photon. J.*, vol. 6, no. 5, Oct. 2014, Art. no. 5501209.

[15] X. Wang, Y. Li, and X. Bao, "C- and L-band tunable fiber ring laser using two-taper Mach-Zehnder interferometer filter," *Opt. Lett.*, vol. 35, no. 20, pp. 3354–3356, 2010.

[16] B. Saxena, Z. Ou, X. Bao, and L. Chen, "Low frequency-noise random fiber laser with bidirectional SBS and Rayleigh feedback," *IEEE Photon. Technol. Lett.*, vol. 27, no. 5, pp. 490–493, Mar. 2015.

[17] L. Wang, X. Dong, P. P. Shum, C. Huang, and H. Su, "Erbium-doped fiber laser with distributed Rayleigh output mirror," *Laser Phys.*, vol. 24, no. 11, 2014, Art. no. 115101.

[18] C.-H. Yeh, H.-Y. Cheng, Y.-C. Chang, C.-W. Chow, and J.-H. Chen, "Silicon-micro-ring resonator based erbium fiber laser with single-longitudinal-mode oscillation," *IEEE Photon. J.*, vol. 10, no. 3, Jun. 2018, Art. no. 7103107.

[19] S. Feng, S. Lu, W. Peng, Q. Li, T. Feng, and S. Jian, "Tunable single-polarization single-longitudinal-mode erbium-doped fiber ring laser employing a CMFBG filter and saturable absorber," *Opt. Laser Technol.*, vol. 47, pp. 102–106, 2013.

[20] C.-H. Yeh, W.-P. Lin, Y.-J. Chang, Y.-R. Xie, C.-M. Luo, and C.-W. Chow, "A selectable single-mode erbium laser with power-flattened output employing dual-Sagnac-ring," *IEEE Access*, vol. 7, pp. 92938–92942, 2019.

[21] S.-K. Liaw, C.-S. Shin, and W.-F. Wu, "Tunable fiber laser using fiber Bragg gratings integrated carbon fiber composite with large tuning range," *Opt. Laser Technol.*, vol. 64, pp. 302–307, 2014.